JOURNAL OF GUIDANCE, CONTROL, AND DYNAMICS
Vol. 18, No. 1, January–February 1995

Classical/H_2 Solution for a Robust Control Design Benchmark Problem

Peter M. Thompson*
Systems Technology, Inc., Hawthorne, California 90250

A two-mass-spring benchmark problem is analyzed and solved. Classical control methods of loop shaping and pole placement are used to translate the design requirements into an optimal cost function. This includes the translation of a requirement for parameter robustness into a desired loop shape. The H_2, equivalently linear quadratic Gaussian, problem is then used to synthesize the controller. The design method is automated by adjusting a small number of intuitive design parameters. The controller is compared against 11 published designs. The controller presented here and one of the published designs are found to be significantly better than the rest.

I. Introduction

A BLEND of classical and optimal control is used to solve the robust control design benchmark problems in Ref. 1. The controlled element is two masses joined by a spring. The masses and spring constants are uncertain, and the basic requirement is to hold the position of one mass, using a force acting on the other, in the presence of disturbances. The problems have received a considerable amount of attention. An early set of solutions is reviewed in Ref. 2, and a different set of solutions is presented in Refs. 3–13. All four benchmark problems are solved here, but most of the attention is directed to the second benchmark problem, which includes a requirement for simultaneous parameter robustness.

There are two ways to rate the solutions to the second problem in Refs. 3–13. The academic criterion is "close is good enough," and the qualitative nature of the requirements supports this point of view. All of the designs come close, and all do an admirable job of demonstrating their respective design methods. The contractual criterion is "the requirements shall be satisfied." There are generally accepted numerical requirements associated with the controller evaluation, and on this basis the 11 designs do not do well:

1) Nine of the designs violate the generally accepted numerical requirements for settling time and/or control level.

2) Eight of the designs have shockingly low gain and/or phase margins.

3) Seven of the designs do not meet parameter robustness specifications.

4) None of the designs satisfy all of the numerical requirements.

The overall impression is that there is considerable room for improvement. The problem specifications are firmed up here by interpreting several of the qualitative requirements as numerical requirements, and a numerical basis for comparing the designs is presented. Two designs emerge as significantly better than the others: the design of Wie[13] and the design presented in this paper. These two differ mainly in the controller bandwidth. If any of the authors feel slighted by the comparison, please accept the numerical requirements as a challenge.

It is relatively easy to devise a numerical scheme to assess controller performance, but it is much harder to rate a design method. It misses the point to make blanket statements like "H_2 is better" or "H_∞ is better" or "(insert your favorite) is better." Important questions are 1) how are the requirements translated into a set of design parameters, 2) how does the adjustment of each design parameter affect the closed-loop system, and 3) are the design parameters decoupled? By decoupled it is meant that each design parameter adjusts a single set ofcompatible requirements or trades off two sets of competing requirements. A design method that rates high in each of these criteria is said to be automated.

The classical and H_2 methods used here work well because they automate the design. My own prejudice is to use classical control first and, only after exhausting this approach, jump to modern techniques. This includes classical multivariable control.[14] Classical control continues to be popular for the simple reason that a very large number of design problems can be automated using classical control. The design parameters are typically the controller gains, poles, and zeros (or numerator and denominator coefficients). The beauty of the benchmark problem is that it appears at first to be the kind of problem that can be automated using classical control, but then turns out not to be. The required controller gains, poles, and zeros are strongly coupled and cannot be separately adjusted to meet individual requirements. The alternative used here is to automate the design by defining an optimal cost function in terms of a small set of design parameters. The design parameters are decoupled, though not perfectly, and some iteration is required to home in on the final design.

Classical control is used to translate the requirements into an optimal cost function. Guidelines for doing so are based on desired loop shapes (Bode magnitude and phase curves) and desired closed-loop pole locations, the very essence of classical control. The cost function consists of 1) a weighted output that shapes the low-frequency portion of the loop transfer function and hence determines performance, 2) a weighted output that damps the uncertain resonant mode and hence increases parameter robustness, and 3) a mid- and high-frequency loop shape that trades off control energy, crossover robustness, and parameter robustness. The guidelines are justified using exact and approximate relationships between the cost function and the resulting closed-loop system. These relationships remove the mystery that so often accompanies the selection of a cost function.

The cost function is minimized using the H_2 norm. The main reason for using H_2 is that analytical relationships between the cost function and the closed-loop system are well established; in particular, loop transfer recovery (LTR) and the optimal root locus. The solution does not use loop transfer recovery, but it comes close. A second reason for selecting the H_2 problem is to show that relatively pedestrian methods can work very well for the benchmark problem. The standard linear quadratic Gaussian (LQG) problem in Ref. 15 is a special case of the H_2 problem, and the cost function developed here falls into this special case. I did not start out by limiting myself to the standard LQG problem; it just turned out that way. I prefer to use the label H_2 because it refers to the more general problem. The types of generalizations that would push the current problem out of the standard LQG realm of applicability are new disturbance inputs, new error outputs, direct weighting of uncertainties, augmented dynamics, and so on.

In Sec. II the controlled element is defined and the requirements for benchmark problems 1 and 2 are stated. The union of these two problems is treated as a single problem. The deficiencies of the controlled element and the extra challenges imposed by parameter

Received Sept. 30, 1993; revision received Jan. 25, 1994; accepted for publication Feb. 25, 1994.

*Principal Specialist. Member AIAA.

changes are analyzed and a strategy for robust control is established. In Sec. III the H_2 problem is defined and the guidelines for selecting the cost function are developed. In Sec. IV the iterative design process is summarized and the resulting closed-loop system is analyzed. A comparison with published benchmark problem solutions is presented in Sec. V. Several alternative designs and the solutions to benchmark problems 3 and 4 are presented in Sec. VI, and brief concluding remarks are provided in Sec. VII.

The following shorthand notation is used for transfer function numerators and denominators:

$$a(s+b)(s^2+2\zeta\omega s+\omega^2)=a(b)[\zeta,\omega]$$

The damping ratio and natural frequency provide more insight than the real and imaginary parts.

II. Control Design Problem

Controlled Element

A two-mass system connected by a spring, as shown in Fig. 1, is a simple model of a dynamic system with a single resonance. A real mechanical system has many resonances, but it is often the case that only a single dominant mode needs to be modeled to provide meaningful insights. The model used here is further simplified by not including any damping or friction and by not including sensor or actuator dynamics. The system and its controller form a translational position control system. Rotational versions are more common and form the basis for many common servomechanisms, including tracking antennas, telescope pointing and tracking systems, and robotic arms.

By equating forces at each mass the following equations are derived:

$$m_1\ddot{x}_1=-k(x_1-x_2)+w_1+u \tag{1a}$$

$$m_2\ddot{x}_2=k(x_1-x_2)+w_2 \tag{1b}$$

The most important transfer function for the design is x_2 in response to u, which is decomposed below into rigid-body and resonant parts:

$$\frac{x_2}{u}=g=g_{\text{rb}}\times g_{\text{res}}=\frac{1/(m_1+m_2)}{s^2}\times\frac{\omega_p^2}{s^2+\omega_p^2} \tag{2}$$

where $\omega_p^2=k(1/m_1+1/m_2)$. A state-space model of the system is

$$\begin{bmatrix}\dot{x}_1\\ \dot{x}_2\\ \dot{x}_3\\ \dot{x}_4\end{bmatrix}=\begin{bmatrix}0 & 0 & 1 & 0\\ 0 & 0 & 0 & 1\\ -k/m_1 & k/m_1 & 0 & 0\\ k/m_2 & -k/m_2 & 0 & 0\end{bmatrix}\begin{bmatrix}x_1\\ x_2\\ x_3\\ x_4\end{bmatrix}$$

$$+\begin{bmatrix}0 & 0\\ 0 & 0\\ 1/m_1 & 0\\ 0 & 1/m_2\end{bmatrix}\begin{bmatrix}w_1+u\\ w_2\end{bmatrix} \tag{3}$$

The outputs of interest are x_1, x_2, and $r=\dot{x}_1-\dot{x}_2=x_3-x_4$. The measured output is $y=x_2+v$, which is corrupted by noise. The output signal r is used in the optimal cost function and forces velocity damping of the resonance. The different parts of the state-space model are labeled as follows:

$$\begin{bmatrix}\dot{x}\\ x_1\\ x_2\\ r\end{bmatrix}=\begin{bmatrix}A & B_u & B_{w_2}\\ C_{x_1} & 0 & 0\\ C_{x_2} & 0 & 0\\ C_r & 0 & 0\end{bmatrix}\begin{bmatrix}x\\ w_1+u\\ w_2\end{bmatrix} \tag{4}$$

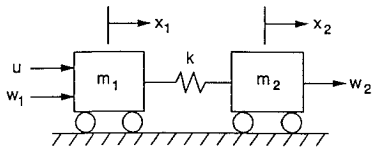

Fig. 1 Two-mass-spring system with uncertain parameters.

Requirements

The purpose of the linear control system is to hold the position x_2 in the presence of disturbances and parameter variations. The position x_2 is measured and used to control the input u. The nominal system has $m_1=m_2=k=1$. The following requirements shall be satisfied:

1) For a unit impulse disturbance exerted on body 1 or body 2, the controlled output of the nominal system shall not exceed 0.1 after 15 time units.

2) For the same disturbances the peak control level of the nominal system shall not exceed 1.

3) The gain margin shall be 6 dB or greater and the phase margin shall be at least 30 deg.

4) The closed-loop system shall be stable for $0.5\le k\le 2.0$ and $m_1=m_2=1$.

5) The closed-loop system shall be stable for simultaneous changes $0.7\le k, m_1, m_2\le 1.3$.

6) There shall be reasonable high-frequency sensor noise rejection, performance robustness, and controller complexity.

These requirements are the union of benchmark problems 1 and 2 from Ref. 1 and are collectively referred to here as benchmark problem 2. The first five requirements are numerical requirements, and the last is a set of qualitative requirements. The control energy and sensor noise requirements are compatible; helping one helps the other. There is a major tradeoff between control energy and all types of robustness and minor tradeoffs between each type of robustness. An absolute threshold is used for the settling time criteria. Some authors have used 10% of the maximum deviation as the threshold, but that view is not adopted here because it rewards large transient errors. Despite the apparent simplicity, this turns out to be a challenging design. Reasons why include that the resonance is close to the required bandwidth frequency, the sensor and actuator are noncollocated, the range of parameter uncertainty is quite large, and the allowable peak control level is severely limited.

A comment on the gain and phase margin requirement is in order. Any good system looks like K/s around the crossover frequency,[14] and the gain and particularly the phase margin are a measure of deviation from this ideal. Traditional requirements are 6 dB and 45 deg. Controlled element uncertainty of ± 3 dB is considered typical, and a 6-dB gain margin provides a safety margin. There are some systems flying about with less than 6 dB, but only after extraordinary efforts have been taken to define the controlled element model. A phase margin requirement is an indirect way of specifying the transient response characteristics; for example, a second-order system with 45 deg of phase margin will have a damping ratio greater than 0.4. A phase margin requirement of 30 deg is sometimes used for regular problems (such as this one), where error rejection is more important than transient response characteristics. Phase margins less than 30 deg have dangerously low tolerance for unmodeled high-frequency dynamics and nonlinearities such as actuator rate limiting.

Ideal Loop Shape

The deficiencies in the controlled element are analyzed and a strategy for robust control is determined. In the low-frequency region, lead compensation is needed to stabilize the rigid body and provide adequate phase margin. In the unit magnitude crossover region, a flat frequency shape minimizes the sensitivity to gain variations, a result from Bode, as reiterated in Ref. 5.

The design cries out for a high-frequency inner loop using rate and/or acceleration measurements to damp the resonance. We will keep within the constraints of the problem, however, and only use the x_2 position measurement, except for a brief look in Sec. VI. The main consequence of the parameter uncertainty is to eliminate the use of highly tuned notch filters. Two classical control approaches for damping movable resonances are to 1) lag the resonance so that, no matter where it is, at least it is small or 2) phase stabilize the resonance by adding zeros below its lowest possible location so that the root locus branches emanating from the resonance head off into the left-half plane and terminate at the zeros. The optimal design takes a compromise approach, although it can be made to favor one or the other.

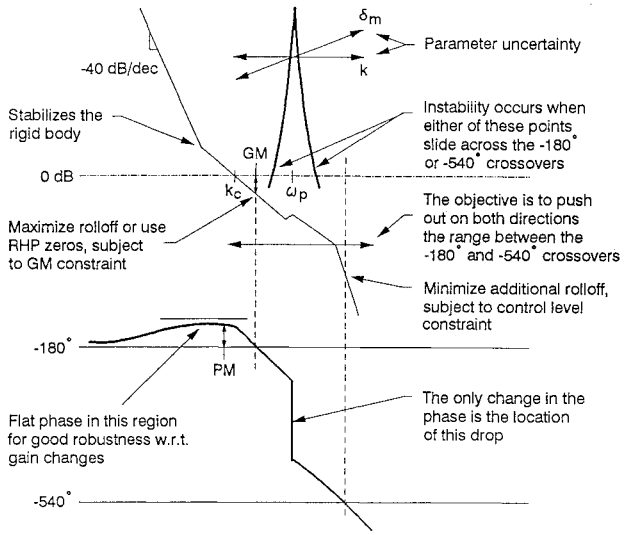

Fig. 2 Guidelines for the loop shape.

Let us now take a close look at the effects of parameter variation. The parameters k, m_1, and m_2 are all uncertain, and the following variables characterize the uncertainty:

δ_m = parameter changes in direction $k + \delta_m, m_1 - \delta_m$, and $m_2 - \delta_m$

p_m = maximum variation such that closed-loop system remains stable for changes $1 - p_m \le k, m_1, m_2 \le 1 + p_m$

The first variable defines a worst-case parameter change, and the second is a simultaneous parameter robustness measure that is used in later sections to analyze the controller. The changes in ω_p are the same for $0.5 \le k \le 2.0$ and $-0.5 \le \delta_m \le 0.5$. The rigid-body gain does not change with k, but changes from -3.5 to $+6.0$ dB with δ_m. A key point is that the only change in the phase of $g(s)$ is the location of the -180 deg phase drop that occurs at ω_p.

Define the controller as $c(s)$; the loop transfer function is $gc(s)$. For the type of controller used here, the phase curve of $gc(s)$ crosses the -180 deg line just before ω_p and crosses the -540 deg just after ω_p. This is illustrated in Fig. 2. The closed-loop system is destabilized when the gain increases above unity at either of these two phase crossover frequencies. Parameter changes that decrease ω_p will eventually cause an instability at the lower crossover frequency, and parameter changes that increase ω_p can cause an instability at either frequency (because increases in δ_m also increase the gain).

Robustness with respect to parameter changes is improved by shifting the -180 deg to the left and shifting the -540 deg to the right. To accomplish this, the phase should 1) decrease rapidly through -180 deg, by increasing the magnitude rolloff or using right-half-plane zeros, subject to the gain margin constraint, and then 2) decrease slowly through -540 deg, by decreasing the additional magnitude rolloff, subject to the control energy constraint.

Different phase shapes from that shown in Fig. 2 are possible. Controllers that lead with three right-half-plane zeros do not have a -180 deg crossover before ω_p and have a -180 deg crossover afterward. These are phase-stabilizing controllers that typically have great robustness but require gross violations of the peak control level requirement. Lagging controllers can be designed that have a -180 deg crossover before ω_p and no -540 deg phase crossover. Such controllers are stable for arbitrarily large increases in k.

III. H_2 Optimal Control Problem

Interconnection Structure

The H_2 optimal control problem allows considerable freedom in defining disturbance inputs, error outputs, and weights and frequency shapes for each. The combination of plant, controller, and weights is called the interconnection structure. The structure for this problem is shown in Fig. 3 and contains the following parts:

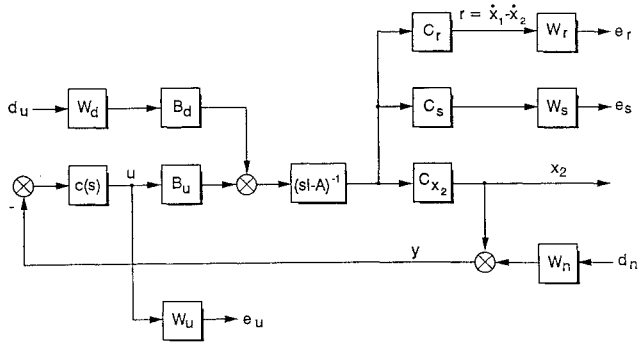

Fig. 3 Interconnection structure.

1) *Performance* (e_s/u): This shapes the high-gain, low-frequency region to achieve the desired crossover frequency.

2) *Damping* (e_r/u): This damps the resonant modes to achieve parameter robustness.

3) *High-frequency rolloff* (x_2/d_u): This shapes the mid- and high-frequency gain to tradeoff control energy, crossover robustness, and parameter robustness.

The interconnection structure is denoted by $M(s)$. A transfer function version is shown below:

$$\begin{bmatrix} e_s \\ e_r \\ e_u \\ \hline y \end{bmatrix} = \left[\begin{array}{ccc|c} W_s\frac{n_{sd}}{\Delta}W_d & 0 & & W_s\frac{n_s}{\Delta} \\ W_r\frac{n_{rd}}{\Delta}W_d & 0 & & W_r\frac{n_r}{\Delta} \\ 0 & 0 & & W_u \\ \hline \frac{n_d}{\Delta}W_d & W_n & & g \end{array}\right] \begin{bmatrix} d_u \\ d_n \\ \hline u \end{bmatrix} \tag{5}$$

The lines separate the signals and corresponding blocks of $M(s)$ into functional groups. Label the blocks M_{11}, M_{12}, M_{21}, and M_{22}. A state-space version of the interconnection structure is

$$\begin{bmatrix} \dot{x} \\ e_s \\ e_r \\ e_u \\ y \end{bmatrix} = \begin{bmatrix} A & B_dW_d & 0 & B_u \\ W_sC_s & 0 & 0 & 0 \\ W_rC_r & 0 & 0 & 0 \\ 0 & 0 & 0 & W_u \\ C_{x_2} & 0 & W_n & 0 \end{bmatrix} \begin{bmatrix} x \\ d_u \\ d_n \\ u \end{bmatrix} \tag{6}$$

The numerators shown in the transfer function version are defined by $n_s/\Delta = C_s(sI - A)^{-1}B$, $n_d/\Delta = C(sI - A)^{-1}B_d$, and so on. The equivalent LQG problem is

$$\dot{x} = Ax + B_u u + W_d B_d d_u \tag{7a}$$

$$y = C_{x_2}x + W_n d_n \tag{7b}$$

$$J = \int_0^\infty \left(e_s^2 + e_r^2 + e_u^2\right) dt \tag{7c}$$

The closed-loop poles of the optimal system are the same as the left-half-plane zeros of the numerators of $M_{12}^{\sim}M_{12}$ and $M_{21}M_{21}^{\sim}$. The closed-loop poles are respectively called controller and observer poles. The tilde operator is defined by $M_{12}^{\sim} = M_{12}^T(-s)$. These numerators are used in the subsequent discussions to determine analytical relationships between the closed-loop poles and the cost functions. These relationships are a practical advantage that the H_2 problem has over the recently more popular H_∞ problem. These numerators can also be used to respectively define controller and observer optimal root loci.

The solution of the H_2 problem finds the optimal controller $c(s)$ that stabilizes the closed-loop system and minimizes the H_2 norm of the error. The two-Riccati-equation solution described in Ref. 16 is used to compute the solution. The actual implementation of the solution is the one contained in Ref. 17.

Guidelines for Selecting Weights

The optimal design amounts to the selection of the following weights and vectors: W_s, W_u, C_s, W_r, W_d, W_n, B_d. Without loss of generality we immediately set $W_u = W_n = 1$. Selecting C_s and B_d is equivalent to selecting the numerators n_s and n_d, respectively. The general relationship is described in the Appendix, and special cases are used throughout this section. The numerators n_{sd} and n_{rd} also depend on C_s and B_d, but we select these vectors based on n_s and n_d and let n_{sd} and n_{rd} fall where they may. Reasons for selecting each of the weights and numerators are now described.

Performance

The optimal loop transfer function $gc(s)$ is approximated in the low-frequency region as follows:

$$gc(j\omega) \approx \frac{e_s}{u}(j\omega) \quad \text{for} \quad \omega \quad \text{such that} \quad \left|\frac{e_s}{u}(j\omega)\right| \gg 1 \tag{8}$$

This approximation holds true if the observer closed-loop poles (determined, as explained later, by W_d and n_d) are placed far enough above the rigid-body and resonant poles. One choice for e_s/u is to keep the double-integrator shape of the rigid-body part of the system:

$$\frac{e_s}{u} = \frac{k_c^2}{s^2} \times g_{\text{res}} \tag{9}$$

where k_c radians per second is the desired crossover frequency. To make this choice, set $W_s = k_c^2(m_1 + m_2)$, $n_s = 1$, and $C_s = C_{x_2}$. The H_2 solution will automatically supply the low-frequency lead required to stabilize the rigid body. The low-frequency lead will push the actual crossover frequency slightly above k_c. The requirements specify settling time, and it is observed empirically that $t_s \approx 4.5/k_c$.

To alter the low-frequency shape of $gc(s)$, a numerator n_s with a single zero can be chosen:

$$\frac{e_s}{u} = \frac{k_c(s+a)}{s^2} \times g_{\text{res}} \tag{10}$$

Set $W_s = k_c(m_1 + m_2)$, $n_s = (s + a)$, and $C_s = C_{x_2}(A + aI)$. The choice $a = \frac{1}{2}k_c$ will create a double pole on the real axis, which helps to reduce the overshoot.

If additional dynamics are needed, they can be included in W_s. For example, if the actual system has friction and zero velocity error is required, then W_s can be augmented with a trim integrator. This is typical of tracking antenna and telescope servocontrol systems. The third benchmark problem asks for sinusoidal disturbance rejection, which is achieved by including a model of this disturbance in W_s.

Damping

The error output $r = \dot{x}_1 - \dot{x}_2$ is used to damp the resonant mode. The intuitive reason for this output is that it forces *velocity damping* while leaving the resonant frequency unchanged. An analytical reason for why this output works can be shown using the numerator of $M_{12}^{\sim}M_{12}$. The error outputs e_s and e_r have been chosen so that the weights W_s and W_r, respectively, determine the closed-loop locations of the rigid-body and resonant modes. The closed-loop resonant mode is the complex left-half-plane zero of the following transfer function:

$$\left(W_r\frac{n_r}{\Delta}\right)^{\sim}\left(W_r\frac{n_r}{\Delta}\right) + 1 = \frac{-(W_r s/m_2)^2}{\left(s^2 + \omega_p^2\right)^2} + 1 \tag{11}$$

After a moderate amount of algebra, which is left to the reader as an exercise, the closed-loop damping ζ_r of the resonant mode is found to be related to the weight W_r by:

$$\zeta_r = \frac{W_r}{2\omega_p\sqrt{m_1}} \tag{12}$$

Substitute for the nominal parameters, and it follows that $W_r = 2.83\zeta_r$.

The H_2 problem is general enough to allow variations in the compliance to be directly weighted. To do this, define $k = k_0 + k_1\Delta_k$, where $|\Delta_k| < 1$, and then insert a disturbance input and error output on either side of the Δ_k. After all is said and done, this amounts to *position damping* of the resonant mode. Position damping is not as desirable as velocity damping, as it provides less damping for a given gain and results in a higher natural frequency. That is why the error output r is defined as $\dot{x}_1 - \dot{x}_2$ and not $x_1 - x_2$.

High-Frequency Rolloff

The observer closed-loop poles are the left-half-plane zeros of the following transfer function:

$$M_{21}M_{21}^{\sim} = \left(W_d\frac{n_d}{\Delta}\right)\left(W_d\frac{n_d}{\Delta}\right)^{\sim} + 1 = \frac{n_{\text{obs}}n_{\text{obs}}^{\sim}}{\Delta\Delta^{\sim}} \tag{13}$$

The design parameters W_d and n_d are used to approximately place the closed-loop poles. A high enough frequency, the closed-loop poles are approximately those of the compensator $c(s)$; hence they shape the high-frequency rolloff of $gc(s)$. The zeros of $c(s)$ also effect the rolloff and are automatically positioned by the H_2 solution. If the rolloff is pushed up to high frequencies, the controller will have high gain and good robustness. If the rolloff is pushed down to ω_p or lower, the opposite is true. The desired compromise is the ideal loop shape detailed in Sec. II.

One choice for the design parameters is $W_d n_d = \omega_b^4$, in which case n_{obs} forms a fourth-order Butterworth pattern with radius ω_b. To make this choice, set $W_d = \omega_b^4$, $n_d = 1$, and $B_d = (m_1m_2/k)B_u$. In this case the LTR result can be applied: as ω_b approaches infinity, $gc(s)$ approaches the loop transfer function obtained using linear quadratic regulator full state feedback. The required conditions, both satisfied, are that the system is non-minimum phase and B_d is proportional to B_u. As fate would have it, this choice is not good enough to meet the requirements of the benchmark problem. The problem is that a fourth-order Butterworth pattern has a sudden dropoff, whereas the ideal loop shape calls for a graduated high-frequency rolloff.

A better choice is on $W_d n_d = \omega_b^2[\zeta_d, \omega_d]$. For high enough ω_b, two poles in n_{obs} are trapped at $[\zeta_d, \omega_d]$, and the remaining two fall into a second-order Butterworth pattern. To achieve this choice, set $W_d = \omega_b^2$, $n_d = [\zeta_d, \omega_d]$, and $B_d = (m_1m_2/k)n_d(A)B_u$. By separately adjusting the two sets of complex observer poles, a good compromise for the high-frequency rolloff can be reached.

Summary of Design Guidelines

Use the interconnection structure defined in Fig. 3. Select the following design parameters:

$$k_c = \text{slightly less than desired rigid-body bandwidth, rad/s} \tag{14a}$$

$$\zeta_r = \text{desired resonant mode damping ratio} \tag{14b}$$

$$n_d = \text{high-frequency rolloff, } [\zeta_d, \omega_d] \tag{14c}$$

$$\omega_b = \text{additional high-frequency rolloff, rad/s} \tag{14d}$$

The relationship between the requirements and design parameters is shown in Table 1.

Table 1 Connections between requirements and design parameters

Requirements	Connections	Design parameters
Performance		k_c
Parameter robustness		ζ_r
Crossover robustness		n_d, ω_b
Control energy		

Set $W_u = W_n = 1$. The preferred choices for the weights and vectors are

$$W_s = k_c^2(m_1 + m_2) \tag{15a}$$

$$C_s = C_{x_2} \tag{15b}$$

$$W_r = 2\zeta_r\omega_p\sqrt{m_1} \tag{15c}$$

$$W_d = \omega_b^2. \tag{15d}$$

$$B_d = \frac{m_1 m_2}{k}\left(A^2 + 2\zeta_d\omega_d A + \omega_d^2 I\right)B_u \tag{15e}$$

The following alternative choices for W_s and C_s result in less overshoot:

$$W_s = k_c(m_1 + m_2) \tag{16a}$$

$$C_s = C_{x_2}\left(A + \tfrac{1}{2}k_c I\right) \tag{16b}$$

IV. Solution to Benchmark Problem 2

Design Iterations

The discussion so far has been about guidelines and the reasons for them. Now the actual design experience is recounted. It was found that a crossover frequency of 0.35 rad/s was needed to meet the 15-s settling time requirement, and setting $k_c = 0.30$ achieved this. The benchmark problem does not specify the damping of the resonant mode. Not very much was required, and to meet the settling time requirement and provide parameter robustness, $\zeta_r = 0.2$ was selected.

Many iterations were required to select suitable values for ω_b and n_d. At each stage of the iteration, the robustness margins were calculated and the u/w_2 impulse response was plotted. Each iteration took less than 1 min to compute and plot and would probably take only seconds on a faster computer. I started with a fourth-order Butterworth pattern and gradually brought the cutoff down in frequency. Everything was fine except for parameter robustness, which is why I abandoned LTR and generalized the method to allow staggered high-frequency poles. I fixed a single pole at different relatively low frequencies and brought third-order Butterworth patterns down in frequency, again without success. Finally a successful compromise was found by fixing the second-order lag at a relatively low frequency and adjusting the second-order Butterworth pattern. Though meticulous, the iterations are much less trouble than directly changing the controller poles and zeros, as would be required using classical control.

The final choice for the design parameters are

$$k_c = 0.3, \qquad \zeta_r = 0.2, \qquad n_d = [0.8, 1.6], \qquad \omega_b = 8 \tag{17}$$

and the corresponding weights and vectors are

$$W_s = 0.18, \qquad W_r = 0.566, \qquad W_d = 64, \qquad B_d = (A^2 + 2.56A + 2.56I)B_u \tag{18}$$

The resulting H_2 optimal controller is

$$c(s) = \frac{122(0.14)[-0.581, 1.32]}{[0.732, 2.42][0.694, 7.99]} \tag{19}$$

The compensator numerator contains a low-frequency zero that stabilizes the rigid-body mode and right-half-plane zeros that damp the resonance. The poles of $c(s)$ provide a staggered high-frequency rolloff. The closed-loop poles are

$$\phi_{cl}(s) = \underbrace{[0.722, 0.3]}_{\text{rigid body}}\underbrace{[0.2, 1.42]}_{\text{resonance}}\underbrace{[0.8, 1.6][0.692, 8]}_{\text{rolloff}} \tag{20}$$

Analysis

At the nominal value of $k = 1$, the phase margin PM = 35 deg, the gain margin GM = 6.1 dB, the settling time $t_s = 14.5$ s, and the maximum control level for unit impulse disturbances is 0.76. The range of stable compliance is $0.44 \le k \le 2.8$, and the parameter robustness measure $p_m = 0.42$. More will be said about p_m in a moment. All of the numerical requirements of the benchmark problem are satisfied.

Figure 4a shows magnitude Bode plots of $gc(s)$ for different levels of δ_m, and Fig. 4b shows corresponding phase curves. The location of ω_p changes, but not the -180 deg and -540 deg crossover frequencies. Figure 4c shows the classical root locus of $gc(s)$. Each of the closed-loop modes is labeled, and the damping of the resonance is clearly seen. Figures 4d and 4e show the response to w_1 and w_2 unit impulses, respectively, for three different values of k. The x_2 response for the nominal k settles to within 0.1 after 14.5 s, and the u response stays below 1. The first oscillation of u/w_2 is very sensitive to the location of the high-frequency rolloff of $gc(s)$.

And now for the reasonableness requirements. The controller order is 4, which is reasonable. Performance robustness is assessed as follows and is also found to be reasonable:

PM > 30 deg	for	$0.44 \le k \le 1.9$
GM > 6 dB	for	$1.00 \le k \le 2.3$
$t_s < 15$ s	for	$0.65 \le k \le 1.9$
$\|u\| < 1$	for	$0.44 \le k \le 2.5$

The x_2/v sensor noise is attenuated by more than 20 dB above 3 rad/s, which is reasonable. The controller has a fair amount of lead; u/v has a 20 dB increase at 8 rad/s and then begins to roll off. A situation may arise where the input is applying force at high frequencies due to the sensor noise, even though this does not result in appreciable movement at the output. This is not desirable and is the biggest criticism of the design. The potential sensor noise problem can be abated by decreasing the design parameter ω_b, but this will decrease the parameter robustness measure p_m. The choice I made in this design was to maximize p_m.

A single number that characterizes robustness with respect to simultaneous parameter changes is p_m, defined in Sec. II. To compute p_m, stability tests were computed at each corner of the square that p_m defines in the k vs $m_1 = m_2$ parameter plane. Structured singular-value tests and real parameter structured singular-value tests gave conservative (lower) estimates of p_m and hence were of no use. The two-dimensional k vs $m_1 = m_2$ parameter plane is shown in Fig. 5. Any combination of k and $m_1 = m_2$ in the area marked stable will result in a closed-loop stable system. At points I and II in Fig. 5, ω_p is increasing, and instability occurs respectively at the -540 deg and -180 deg crossover frequencies. At points III and IV, ω_p is decreasing, and instability occurs in both cases at the -180 deg crossover frequency. The $p_m = 0.42$ square does a reasonable job of covering the lower left-hand portion of the stable area but is very conservative for the case of simultaneous increases in both k and $m_1 = m_2$. Further analysis not shown here indicates that mass imbalances up to $\pm p_m$ are guaranteed not to cause instability, and considerably larger mass imbalances are also acceptable.

V. Comparison with Published Solutions

We now compare controller (19) in Sec. IV with the solutions in Refs. 3–13, all of which appear in the same issue of the *Journal of Guidance, Control, and Dynamics*. The surveyed solutions solve benchmark problem 2, or the closest available problem. A scoring system based on a set of numerical requirements and equally weighted deviations, is defined in Table 2 and the next paragraph. The authors, methods, and controllers are listed according to their score in Table 3. Numerical surveys are listed in Table 4.

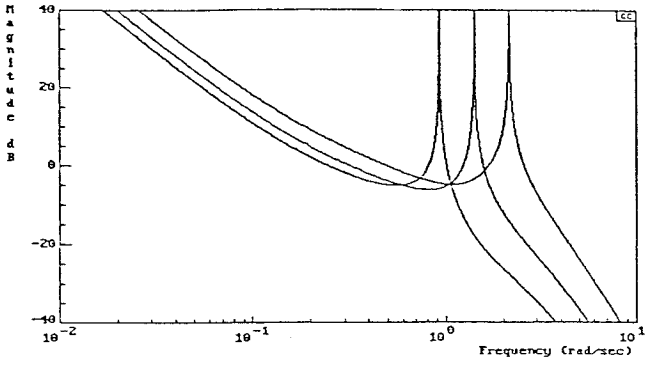

a) $gc(s)$ for $\delta m = -.4, 0, -.4$

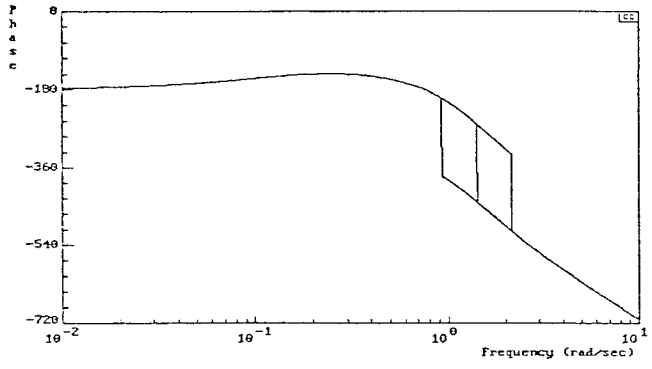

b) Phase

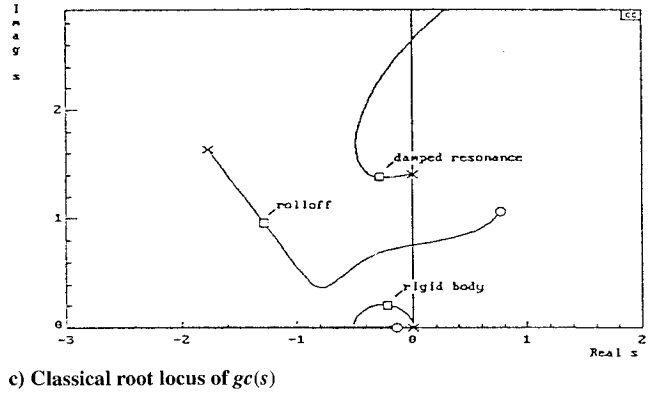

c) Classical root locus of $gc(s)$

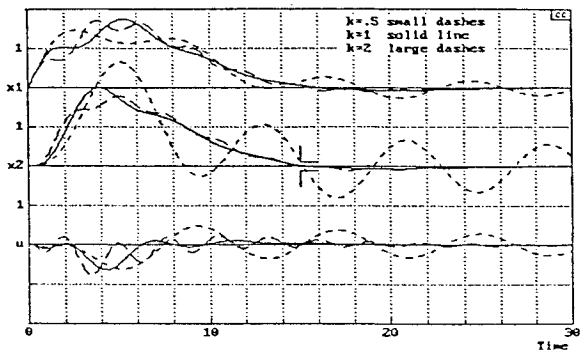

d) $w1$ impulse response

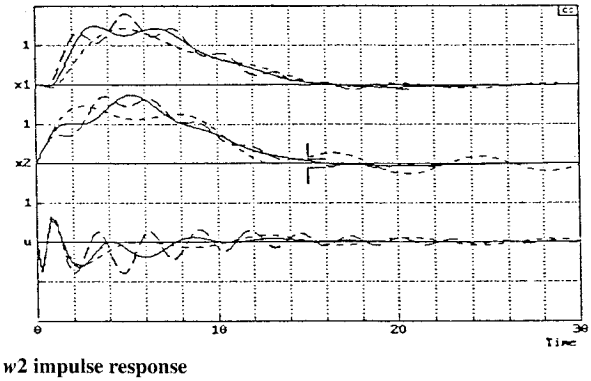

e) $w2$ impulse response

Fig. 4 Graphical survey of H_2 optimal controller (19).

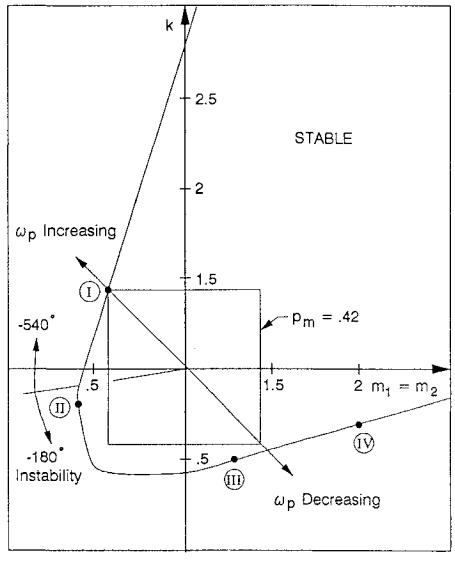

Fig. 5 k vs $m_1 = m_2$ parameter plane.

If a numerical requirement in Table 2 is exactly satisfied, then the score for that requirement is zero. Deviations are scaled so that each is worth ± 1 point. The score for each requirement is limited to ± 2 points, except for the control level, which is limited above by $+2$ points but is not limited from below. A bonus of 2 points is awarded if all of the requirements are satisfied. The total score is calculated as

$$\lim[(\mathrm{PM} - 30)/5] + \lim[(\mathrm{GM} - 6)/2] + \lim[(t_s - 15)/3] + \mathrm{upperlim}[-(20\log_{10} u_{\max})/3] + \lim[(p_m - 0.3/0.05] + \lim[(20\log_{10}(k_{\max}/k_{\min}) - 12)/3] + \mathrm{bonus} \quad (21)$$

In this scoring system a total score of zero is good, a score over $+4$ is very good, and a score below -4 indicates the design needs improvement. If all of the requirements are exactly satisfied, then the total score equals the bonus. The scoring system allows you to trade off requirements, but by doing so you lose the bonus. Penalties for missing an individual requirement are not too harsh, and extravagantly exceeding a single requirement does not gain you much. A penalty of -2 is accessed for each doubling of the peak control level. The penalty for violating the peak control level is not limited because the easiest way to satisfy all of the other requirements is to rev up the control. Three of the designs take this approach.

The designs fall into the following categories:

1) *Very good* (designs 1 and 2): The design presented in this paper is the only one that satisfies all of the numerical requirements. It achieves the highest score of $+7.4$. If not for losing the bonus by 0.2 s, the second-place design would be the best. These two designs are further compared in Sec. VI.

2) *Good* (designs 3–7): These do not make it into the top tier because each has sacrificed crossover robustness, three miss the settling time, and two violate the peak control level.

3) *Needs improvement* (designs 8–12): These designs are penalized for using too much control, for missing several requirements without a corresponding benefit, or both.

Table 2 Numerical requirements and equally weighted deviations

Variable	Definition	Requirement	Deviation
PM	Phase margin	30 deg	5 deg
GM	Gain margin	6 dB	2 dB
t_s	$\lvert x_2(t)1 < 0.1$ for $t \geq t_s$	15 s	3 s
$u_{\max}$	$\max \lvert u(t) \rvert$	1	−3 dB
$k_{\max}/k_{\min}$	Stable for $k_{\min} \leq k \leq k_{\max}$	$0.5 \leq k \leq 2$	3 dB
p_m	Stable for $1 - p_m \leq k, m_1, m_2 \leq 1 + p_m$	0.3	0.05

Table 3 Solutions to benchmark problem 2, ordered by score

Design	Reference	Method	Controller
1	17, Eq. (19) in this paper	Classical and H_2	$c_s = \dfrac{122(0.14)[-0.581, 1.32]}{[0.732, 2.42][0.694, 7.99]}$
2	13, Eq. (40)	H_∞	$c(s) = \dfrac{-0.241(0.132)(1.07)(-3.88)}{[0.877, 0.857][0.341, 1.57]}$
3	5, next eq. after (5)	Approx. pole placement	$c(s) = \dfrac{-1.47(0.0868)(-0.375)}{[0.755, 1.28]}$
4	8, Eqs. (29–32)	μ-Synthesis	$c(s) = \dfrac{14.3(0.139)[-0.954, 1.87]}{[0.39, 2.72][0.951, 3.17]}$
5	11, Eq. (32)	H_∞	$c(s) = \dfrac{116(0.155)(-0.561, 1.18]}{[0.467, 3.26][0.934, 4.67]}$
6	10, Eq. (45)	LTR and H_∞	$c(s) = \dfrac{6.57(0.168)(-1.43)(-3.78)}{[0.682, 1.66][0.365, 4.55]}$
7	12, Eq. (43)	LQG and H_∞	$c(s) = \dfrac{23.3(0.0969)(-0.406)(-4.21)}{[0.303, 3.21][0.881, 3.27]}$
8	4, 2 eqs. after (31)	Game theory	$c(s) = \dfrac{-1190[-0.217, .415][-0.347, 5.26](-26.8)}{[0.285, 3.11][0.891, 3.67][0.702, 11.2]}$
9	9, Eq. (A3)	μ-Synthesis	$c(s) = \dfrac{4.7 \times 10^4(0.22)[0.0856, 0.783][0.104, 5.56](99.9)}{[0.176, 5.85][0.936, 23.3][0.991, 53.9]}$
10	3, Eq. (37)	Minimax LQG	$c(s) = \dfrac{6.15(0.22)[-0.102, 1.64]}{(1.15)[0.154, 2.27](2.43)}$
11	7, bottom of p. 1099	Maximum entropy	$c(s) = \dfrac{2.94 \times 10^6[0.5, 0.08][0.61, 0.508](0.938)}{[0.422, 0.0345](18.8)[0.5, 20](54.8)}$
12	6, Eq. (8)	Quantitative feedback	$c(s) = \dfrac{7.53 \times 10^5(0.66)[0.355, 0.813](2.24)}{[0.925, 5.88](6.66)[0.375, 40]}$

Table 4 Survey of benchmark solutions

Design	PM, deg	GM, dB	t_s, s	$u_{\max}$,	$k_{\min} \rightarrow k_{\max}$	p_m	Meets all?	Score
Requirements	30	6.0	15.0	1	$0.5 \rightarrow 2.0$	0.30		
1	35	6.1	14.5	0.75	$0.44 \rightarrow 2.8$	0.44	Yes	7.4
2	34	6.1	**15.2**	0.57	$0.44 \rightarrow 3.9$	0.45	No	6.4
3	**24**	**3.7**	**29**	0.55	$0.23 \rightarrow \infty$	0.34	No	0.2
4	**27**	**2.8**	14.0	0.95	$\mathbf{0.57 \rightarrow 2.5}$	0.37	No	0.0
5	30	**4.1**	11	**1.35**	$0.50 \rightarrow 2.1$	**0.29**	No	−0.5
6[a]	**23**	**3.1**	14.2	0.88	$\mathbf{0.51 \rightarrow 3.6}$	0.30	No	−0.6
7	**25**	**3.4**	**28**	**1.24**	$0.31 \rightarrow 2.6$	0.36	No	−1.7
8[b]	**25**	**3.2**	**32**	**1.6**	$0.48 \rightarrow 2.0$	**0.27**	No	−6.2
9	60	18	9.0	**500**	$0.27 \rightarrow 7.7$	0.55	No	−8.0
10	**19**	**2.4**	**22**	0.70	$\mathbf{0.68 \rightarrow 1.5}$	**0.19**	No	−8.5
11	31	**5.7**	5.0	**680**	$\mathbf{0.11 \rightarrow 1.9}$	**0.20**	No	−16.8
12	**11**	**2.5**	5.0	**360**	$\mathbf{0.18 \rightarrow 1.3}$	**0.09**	No	−19.1

Note: numbers violate requirements.
[a]Benchmark problem 1.
[b]Benchmark problem 3.

No attempt has been made to rate how well automated the design methods are. All of the scores are based solely on the controllers reported by authors.

VI. Alternative Designs

Five alternatives to controller (19) in Sec. IV are now presented. The first three mimic designs created using other methods, the fourth is a minimum-phase design, and the fifth is a classical design using both x_2 and $\dot{x}_1$ feedbacks. Two more designs are presented that are solutions to benchmark problems 3 and 4 of Ref. 1. A numerical analysis of these seven designs is in Table 5.

Alternative 1: Maximizing Robustness

The high-frequency rolloff is pushed out well beyond the rigid-body crossover frequency. In order for this to be an allowable design, the peak control level requirement must be considerably increased.

Table 5 Survey of alternative designs

Alternate design	PM, deg	GM, dB	t_s, s	u_{max}	$k_{min} \rightarrow k_{max}$	p_m	Meets all?	Score
1	55	16	10.4	**67**	$0.35 \rightarrow 5.3$	0.48	no	−2.6
2	30	**4.0**	14.1	0.78	$0.47 \rightarrow \infty$	0.36	no	3.2
3	32	6.1	15.0	0.56	$0.37 \rightarrow 2.5$	0.42	yes	7.6
4	35	6.1	13.6	0.60	$\mathbf{0.52} \rightarrow \infty$	0.37	no	6.4
5[a]	62	14	11.8	1.00	$0.20 \rightarrow \infty$	0.80	yes	11.1
6[b]	37	**4.6**	**19.7**	0.95	$\mathbf{0.60} \rightarrow \mathbf{2.2}$	0.30	no	−1.0

Note: numbers violate requirements.
[a]Uses velocity feedback.
[b]Benchmark problem 3.

The design parameters and resulting optimal controller are

$$k_c = 0.4, \qquad \zeta_r = 0.5, \qquad n_d = s + 8, \qquad \omega_b = 16 \tag{22}$$

$$c(s) = \frac{7.1 \times 10^4 (0.214)[-0.0457, 0.83]}{[0.964, 13.7][0.483, 16.2]} \tag{23}$$

The peak control level is 67, but the phase margin, gain margin, and settling time requirements are satisfied for $0.5 \leq k \leq 2.8$. The controller has a complex zero almost on the imaginary axis. This is a reasonable location from a classical control point of view. It effectively mimics the locked rotor zero (the zero of x_1/u) and hence phase stabilizes the resonant mode. This design is similar to the μ-synthesis design in Ref. 9, except that here the peak control level is one-eighth as large.

Alternative 2: Quadratic Lag Design

The midfrequency rolloff is pushed down perilously close to the rigid-body bandwidth. In order for this to be an allowable design, the gain margin requirement must be relaxed. The design parameters and resulting optimal control are

$$k_c = 0.3, \qquad \zeta_r = 0.2, \qquad n_d = [0.5, 0.9], \qquad \omega_b = 100 \tag{24}$$

$$c(s) = \frac{170(0.136)(-0.912)(-69.2)}{[0.663, 1.43][0.707, 100]}$$

$$\approx \frac{-1.17(0.136)(-0.912)}{[0.663, 1.43]} \tag{25}$$

The second-order Butterworth pattern is set very high so that the controller can be truncated down to second-order. The controller has the familiar lead term to stabilize the rigid body, and the complex pole is a quadratic lag structural filter. The quadratic lag by itself stabilizes the resonance but does not provide enough damping. The optimal design uses a right-half-plane zero to increase the damping of the resonant mode. The main problem with this design is the low gain margin, only 4.0 dB for the nominal parameter values. The performance gets a bit ragged at the lower end of the compliance range. The maximum deviation in the position x_2, although not specified, is starting to get large. This design is similar to the approximate pole placement design in Ref. 5, except that here the settling time meets the requirement.

Alternative 3: Second-Place Design

The controller in Ref. 13 comes in second place in Table 5 (just barely). The pole/zero constellation of the controller is quite a bit different from that of Eq. (19), and the comparison is interesting. I repeated the design using my method and in the process removed the one smidgen of trouble that their design has with settling time. The result is

$$k_c = 0.9, \qquad n_s = s + 0.45, \qquad \zeta_r = 0.2, \qquad n_d = [0.6, 0.7], \qquad \omega_b = 0.725 \tag{26}$$

$$c(s) = \frac{-0.282(0.127)(2.32)(-2.52)}{[0.882, 1.02][0.303, 1.72]} \tag{27}$$

The design parameters n_d and ω_b are set low to create two midfrequency quadratic lags. In order to prevent excessive phase lag, the H_2 solution automatically shifts the midfrequency zeros to the right- and left-half-plane on the real axis. All of the low control level designs have a tendency to overshoot, so I adjusted k_c and n_s to decrease the overshoot. The numerical requirements are all satisfied.

This design has the advantages of lower peak control levels, slightly better performance at low compliance, and better sensor noise rejection. Controller (19) has the advantages of less transient deviation in the x_2 response, better damping, and slightly better performance at high compliance. The main difference between this controller and that of Eq. (19) is the controller bandwidth. This one begins to roll off at 1.7 rad/s, vs 8 rad/s. At 10 rad/s, $gc(s)$ using this controller is −110 dB, vs −60 dB. The resonant dynamics above the fundamental have not been modeled, but because this controller (and that in Ref. 19) has significantly less gain above 1.7 rad/s, there is less of a chance for spillover problems. For this reason many designers would prefer this design.

Alternative 4: Minimum-Phase Controller—With a Surprise

The previous design placed two quadratic lags at midfrequencies. A variation on this approach is shown below:

$$c(s) = \frac{0.903(0.143)(0.859)}{[0.912, 0.746][0.322, 1.51]} \tag{28}$$

This is the best minimum-phase controller that I have seen for the benchmark problem. It would be the best controller of any kind except that the performance gets a bit ragged at low compliance levels. The stability requirement for $0.5 \leq k \leq 2.0$ is missed by 0.02 at the low end. All of the other numerical requirements are satisfied.

And now for the surprise. The closed-loop system has two sets of double complex poles! The root locus is impressive. This controller was generated using the transfer function pole placement routine in Ref. 17 with the closed-loop poles $\phi_{cl}(s) = [0.8, 0.42]^2[0.18, 1.37447]^2$.

Alternative 5: Classical Controller Using Velocity Feedback

Now we step out of the bounds imposed by benchmark problem 2 and use both position and velocity feedback. Define the following classical control law:

$$u = -k_{\dot{x}_1}\left(\dot{x}_1 + k_{x_2} x_2\right) \tag{29}$$

The inner velocity loop damps the resonant mode, and the outer position loop establishes the performance. The velocity of the first mass is used because this location is collocated with the actuator. Use sequential loop closures to respectively determine $k_{\dot{x}_1} = 1$ and $k_{x_2} = 0.2$. The controller has no dynamics, yet the performance and robustness are phenomenal, at least when compared to designs using only x_2 feedback. The system is stable for $k \geq 0.2$ and $p_m = 0.8$, and the gain and phase margins, settling time, and peak control level requirements are all satisfied for $k \geq 0.53$. These are all very strong reasons to use velocity damping. Options for this design are 1) add an integrator to the outer loop to help overcome friction, 2) add an integrator to the inner loop for velocity command following with zero error with the outer loop open, 3) derive the velocity

measurement from an accelerometer placed on the first mass, and 4) add accelerometers on both masses to derive $r = \dot{x}_1 - \dot{x}_2$ and increase the resonant mode damping.

Benchmark Problem 3

Add the following requirement: A sinusoidal disturbance at 0.5 rad/s with unknown amplitude and phase acts on body 1 and/or body 2, and the closed-loop system shall achieve asymptotic disturbance rejection with a 20-s settling time for $0.5 \leq k \leq 2.0$ and $m_1 = m_2 = 1$. Use the same interconnection structure to solve this problem, but multiply W_s by

$$W_{\sin} = \frac{[0.7, 0.5]}{[0.0, 0.5]} \tag{30}$$

The denominator is an internal model of the disturbance, and the numerator helps to damp the resulting compensator pole at $s^2 + 0.25$. The design parameters and resulting compensator are

$$k_c = 0.64, \qquad n_s = s + 0.32, \qquad \zeta_r = 0.15, \qquad n_d = [0.7, 0.7], \qquad \omega_b = 8 \tag{31}$$

$$c(s) = \frac{135(0.0915)[-0.432, 1.25]}{[0.676, 2.21][0.699, 7.99]} \times \frac{[-0.102, 0.406]}{[0, 0.5]} \tag{32}$$

The low frequency is shaped to reduce overshoot, the first quadratic lag is set low to keep the control energy in check, and the second quadratic lag is set high to increase the parameter robustness. The new quadratic dipole pair in the compensator provides the required sinusoidal disturbance rejection. The settling time and peak control level listed in Table 5 are for impulsive inputs. For w_1 or w_2 equal to $\sin(0.5t)$, the values change to $t_s = 19.5$ and $\mu_{\max} = 1.0$. For w_1 or w_2 equal to $\cos(0.5t)$, $t_s = 19.2$ and $u_{\max} = 1.0$.

The requirements for benchmark problem 3 are not satisfied. The choice made here is to keep the control level low and the settling time fast (the 20-s settling time for sinusoidal inputs is satisfied, but not the 15-s time for impulsive inputs.) Parameter changes that decrease ω_p cause trouble. The gain margin is only 4.6 dB and the range of stable compliance is $0.6 \leq k \leq 2.2$. The range can be decreased below 0.5 by further lowering the gain margin and slowing down the response. If higher peak actuator levels are allowed, then the robustness measures can be significantly improved.

Benchmark Problem 4

The last design solves benchmark problem 4 in Ref. 1. Remove the requirement for sinusoidal disturbance rejection, and add a requirement for step response command following with minimal overshoot and minimal settling time. The following control law will do the job:

$$u = c(s)[-x_2 + f(s)x_c] \tag{33}$$

Use $c(s)$ from Eq. (19), and hence the robustness and disturbance rejection analysis is the same as for this earlier design. To reduce overshoot, the prefilter should cancel the low-frequency part of the closed-loop system and not excite the resonance. The first-order prefilter $f(s) = 0.14/s + 0.14$ does this. It can be implemented without dynamics by feedforwarding into $c(s)$. The overshoot is 4%, the peak control level is 0.11, and the shape of the step response is insensitive to parameter changes in the controlled element. The down side is that the 5 and 2% settling times are a rather long 12.2 and 22.2 s.

The prefilter $f(s) = 1.56[0.7, 0.3]/(0.14)(1.0)^2$ cancels more of the low-frequency closed-loop system and then rolls off with a double pole. The rolloff is set to maximize the rise time subject to the peak control level constraint. The peak control level is 0.86, the overshoot is 3%, and the 5 and 2% settling times are 9.3 and 13.6 s, respectively. The cancellation of [0.7, 0.3] will not be exact due to mass variations, but the changes in ω_p are more significant. The resonant mode is more strongly excited by this prefilter and hence is more prominent in the step response. For off-nominal cases, the first prefilter is the preferred choice.

VII. Conclusions

The H_2 (equivalently LQG) optimal control problem is used to design a controller that satisfies the requirements for a robust control benchmark problem. Traditional classical control methods are used to analyze the controlled element and to develop guidelines for selecting the optimal cost function. Contributions in this paper include translating the parameter robustness requirement into a desired loop shape and automating the design by defining a small number of cost function design parameters.

Appendix: Computing a State-Space Input or Output Vector to Match a Numerator

Define $C(sI - A)^{-1}B = a(s)/\Delta(s)$ to be an nth-order, single-input, single-output state space system. Given C and A, the problem is to find the input vector B that results in the desired numerator $a(s)$. Similarly, given B and A, find the output vector C that matches the numerator. Fadeeva's method is used to convert from a state-space system to a transfer function. Fadeeva's method states that

$$a(s) = CN(s)B = a_1 s^{n-1} + \cdots + a_{n-1}s + a_n \tag{A1}$$

$$\Delta(s) = s^n + d_1 s^{n-1} + \cdots + d_{n-1}s + d_n \tag{A2}$$

$$N(s) = \Delta(s)(sI - A)^{-1} = s^{n-1}N_0 + \cdots + sN_{n-2} + N_{n-1} \tag{A3}$$

where $N_0 = I$ and, for $i = 1, \ldots, n$,

$$d_i = \frac{-1}{i}\operatorname{tr}(N_{i-1}A), \qquad N_i = N_{i-1}A + d_i I \tag{A4}$$

Now turn Fadeeva around. If B is unknown, expand $a(s) = CN(s)B$, solve for each polynomial coefficient, and it follows that

$$B' = [a_1 \cdots a_n] \times [(CN_0)' \cdots (CN_{n-1})']^{-1} \tag{A5}$$

Similarly, if the output vector C is the unknown, it follows that

$$C = [a_1 \cdots a_n] \times [N_0 B \cdots N_{n-1}B]^{-1} \tag{A6}$$

References

[1]Wie, B., and Bernstein, D. S., "Benchmark Problems for Robust Control Design," *Journal of Guidance, Control, and Dynamics*, Vol. 15, No. 5, 1992, pp. 1057–1059.

[2]Stengel, R. F., and Marrison, C. I., "Robustness of Solutions to a Benchmark Control Problem," *Journal of Guidance, Control, and Dynamics*, Vol. 15, No. 5, 1992, pp. 1060–1067.

[3]Mills, R. A., and Bryson, A. E., Jr., "Parameter-Robust Control Design Using a Minimax Method," *Journal of Guidance, Control, and Dynamics*, Vol. 15, No. 5, 1992, pp. 1068–1075.

[4]Rhee, I., and Speyer, J. L., "Application of a Game Theoretic Controller to a Benchmark Problem," *Journal of Guidance, Control, and Dynamics*, Vol. 15, No. 5, 1992, pp. 1076–1081.

[5]Lilja, M., and Astrom, K. J., "Approximate Pole Placement Approach," *Journal of Guidance, Control, and Dynamics*, Vol. 15, No. 5, 1992, pp. 1082–1086.

[6]Jayasuriya, S., Yaniv, O., Nwokah, O. D. I., and Chait, Y., "Benchmark Problem Solution by Quantitative Feedback Theory," *Journal of Guidance, Control, and Dynamics*, Vol. 15, No. 5, 1992, pp. 1087–1093.

[7]Collins, E. G., Jr., King, J. A., and Bernstein, D. S., "Application of Maximum Entropy/Optimal Projection Design Synthesis to a Benchmark Problem," *Journal of Guidance, Control, and Dynamics*, Vol. 15, No. 5, 1992, pp. 1094–1102.

[8]Braatz, R., and Morari, M., "Robust Control for a Noncollocated Spring-Mass System," *Journal of Guidance, Control, and Dynamics*, Vol. 15, No. 5, 1992, pp. 1103–1110.

[9]Chiang, R. Y., and Safonov, M. G., "H^∞ Synthesis Using a Bilinear Pole Shifting Transform," *Journal of Guidance, Control, and Dynamics*, Vol. 15, No. 5, 1992, pp. 1111–1117.

[10]Byrns, E. V., Jr., and Calie, A. J., "Loop Transfer Recovery Approach to H_∞ for the Coupled Mass Benchmark Problem," *Journal of Guidance, Control, and Dynamics*, Vol. 15, No. 5, 1992, pp. 1118–1124.

[11]Wang, Y. J., Shieh, L. S., and Sunkel, J. W., "Observer-Based Robust H_∞ Control Laws for Uncertain Linear Systems," *Journal of Guidance, Control, and Dynamics*, Vol. 15, No. 5, 1992, pp. 1125–1133.

[12]Adams, R. J., and Banda, S. S., "Combined Linear Quadratic Gaussian and H_∞ Control of a Benchmark Problem," *Journal of Guidance, Control, and Dynamics*, Vol. 15, No. 5, 1992, pp. 1134–1139.

[13]Wie, B., Liu, Q., and Byun, K.-W., "Robust H_∞ Control Synthesis Method and Its Application to Benchmark Problems," *Journal of Guidance, Control, and Dynamics*, Vol. 15, No. 5, 1992, pp. 1140–1148.

[14]McRuer, D. T., Ashkenas, I. L., and Graham, D., *Aircraft Dynamics and Automatic Control*, Princeton Univ. Press, Princeton, NJ, 1973.

[15]Athans, M., "The Role and Use of the Stochastic Linear-Quadratic-Gaussian Problem in Control System Design," *IEEE Transactions on Automatic Control*, Vol. AC-16, No. 6, 1971, pp. 529–552.

[16]Doyle, J. C., Glover, K., Khargonekar, P., and Francis, B., "State Space Solutions to Standard H_2 and H_∞ Control Problems," *IEEE Transactions on Automatic Control*, Vol. AC-34, 1989, pp. 831–847.

[17]Thompson, P. M., *Program CC Version 4 Reference Manual*, Systems Technology, Inc., Hawthorne, CA, 1988.